

## Extreme Temperatures in the Antarctic

JOHN TURNER,<sup>a</sup> HUA LU,<sup>a</sup> JOHN KING,<sup>a</sup> GARETH J. MARSHALL,<sup>a</sup> TONY PHILLIPS,<sup>a</sup> DAN BANNISTER,<sup>a</sup> AND STEVE COLWELL<sup>a</sup>

<sup>a</sup>British Antarctic Survey, Natural Environment Research Council, Cambridge, United Kingdom

(Manuscript received 13 July 2020, in final form 6 November 2020)

**ABSTRACT:** We present the first Antarctic-wide analysis of extreme near-surface air temperatures based on data collected up to the end of 2019 as part of the synoptic meteorological observing programs. We consider temperatures at 17 stations on the Antarctic continent and nearby sub-Antarctic islands. We examine the frequency distributions of temperatures and the highest and lowest individual temperatures observed. The variability and trends in the number of extreme temperatures were examined via the mean daily temperatures computed from the 0000, 0600, 1200, and 1800 UTC observations, with the thresholds for extreme warm and cold days taken as the 5th and 95th percentiles. The five stations examined from the Antarctic Peninsula region all experienced a statistically significant increase ( $p < 0.01$ ) in the number of extreme high temperatures in the late-twentieth-century part of their records, although the number of extremes decreased in subsequent years. For the period after 1979 we investigate the synoptic background to the extreme events using ECMWF interim reanalysis (ERA-Interim) fields. The majority of record high temperatures were recorded after the passage of air masses over high orography, with the air being warmed by the foehn effect. At some stations in coastal East Antarctica the highest temperatures were recorded after air with a high potential temperature descended from the Antarctic plateau, resulting in an air mass 5°–7°C warmer than the maritime air. Record low temperatures at the Antarctic Peninsula stations were observed during winters with positive sea ice anomalies over the Bellingshausen and Weddell Seas.

**KEYWORDS:** Atmosphere; Antarctica; Antarctic Oscillation; Climate variability; Temperature

### 1. Introduction

Antarctica is a land of extremes. It is the highest, coldest, driest, and windiest continent on Earth, but with a wide range of climatic conditions from the relatively warm, maritime northern part of the Antarctic Peninsula to the frigid plateau of East Antarctica (King and Turner 1997).


Vostok station [78.5°S, 106.9°E; 3488 m above mean sea level (m MSL)] on the East Antarctic plateau recorded the lowest surface temperature observed on Earth when, on 21 July 1983, the temperature fell to  $-89.2^{\circ}\text{C}$ . Analysis of this event (Turner et al. 2009) showed that the very low temperature occurred as a result of the isolation of the station from relatively warm maritime air masses for a period of 10 days. However, it was suggested that even lower temperatures could occur at higher elevations, such as Dome A (4093 m MSL; 80.37°S, 72.35°E) and these have subsequently been identified using satellite observations and automatic weather station (AWS) data (Scambos et al. 2018).

At the other extreme, it has recently been confirmed (Skansi et al. 2017) that the highest surface temperature measured south of 60°S was 19.8°C, recorded at Signy station (60.7°S, 45.6°W; 5 m MSL), South Orkney Islands, on 30 January 1982. Analysis of this event (King et al. 2017) showed that the high temperature occurred when warm midtropospheric air descended to the station during a foehn event as a northerly airstream flowed over the high orography of Coronation Island. On 24 March 2015, Esperanza station

(63.4°S, 57.0°E; 13 m MSL) near the northern tip of the Antarctic Peninsula, recorded a temperature of 17.5°C, which was the highest accepted temperature measured on the Antarctic continent and nearby islands (Bozkurt et al. 2018; Skansi et al. 2017). More recently, Esperanza reported a temperature of 18.3°C on 6 February 2020, although this measurement has yet to be verified.

These four extreme events have received extensive publicity, but there has been little research into extreme temperatures at other Antarctic locations. A record high temperature at South Pole in 1957 was examined by Alvarez and Lieske (1960) and attributed to warm-air advection from the coastal region over several days. A further event that gave record high temperatures at several stations in 1978 was documented by Sinclair (1981), and again linked to advection of warm air into the interior of the continent. More recently, studies have shown that such intrusions of maritime air onto the Antarctic plateau can be well represented by numerical analyses (Nicolas and Bromwich 2011), indicating that the operational analyses can be of value in investigating extremes.

Orcadas station on the South Orkney Islands northeast of the tip of the Antarctic Peninsula and north of the Weddell Sea has Antarctica's longest meteorological record, starting in 1903. Although the early observations have yet to be digitized, daily mean temperatures are available and trends in these mean values and the extremes have been investigated by Zazulie et al. (2010). They found that since 1950 there had been a reduction in the number of cold extremes, particularly in fall and winter. The positive trend in the summer warm

 Denotes content that is immediately available upon publication as open access.

Corresponding author: John Turner, jtu@bas.ac.uk

DOI: 10.1175/JCLI-D-20-0538.1

© 2021 American Meteorological Society



This article is licensed under a Creative Commons Attribution 4.0 license (<http://creativecommons.org/licenses/by/4.0/>).

extremes since 1970 was twice the magnitude of that in the earlier part of the record, indicating the potential impact of stratospheric ozone depletion.

A knowledge of extreme conditions, including their frequency and the synoptic background to the events, is important for ensuring the physical maintenance and safety of the stations, but is also of great research interest, as extreme conditions can contribute significantly to the breakup of ice shelves during the summer months (Scambos et al. 2004). High temperature events can be associated with significant amounts of precipitation, which are important in the interpretation of the signals in ice cores (Schlosser et al. 2016; Turner et al. 2019a). Extreme atmospheric conditions can also have an impact on the formation and melting of sea ice, which in turn can affect the ocean environment (Turner et al. 2017).

There are different interpretations as to what constitutes an extreme event. Determining a suitable definition often depends on the application or reason for considering meteorological parameters that are well beyond the mean. For applications concerned with economic and social impacts, a temperature threshold that leads to physical hardship to certain sections of the community may be appropriate. In tropical areas a threshold temperature of 35° or 40°C can be appropriate because of the societal impacts (Zhai and Pan 2003), with such temperatures occurring on several days or more being very important. In the Antarctic, temperatures above the freezing point are particularly important because of the resultant ice melt and impact on the terrestrial biota (Wake and Marshall 2015). Other investigations of extremes have focused on temperatures above or below a specified percentile, with the 5th and 95th percentiles often being used (Cardil et al. 2014). In other cases an extreme temperature has been taken as a value beyond 2 standard deviations of the mean (Vavrus et al. 2006), but this is of most value if the data have a normal frequency distribution, which, as we show in this paper, is not the case for most Antarctic temperature data.

While there have been a number of climatological studies into extreme temperatures in the extrapolar regions, very few have considered Antarctica. Wei et al. (2019) examined changes in extreme temperatures over 1970–2013 using daily maximum and minimum temperatures, but these quantities are not generally available digitally for Antarctic stations prior to 2000: thus, data from only four stations were available to calculate trends for 1970–2000. In addition, they did not examine the synoptic background to extreme temperature events. Here we therefore consider Antarctic extreme temperatures using all the synoptic observations available from 17 stations with long records. Clearly, slightly higher or lower temperatures will have occurred between the standard observing times and extremes outside the normal reporting times are noted where known. However, the use of the temperatures from the standard reporting hours allows the investigation of the frequency of extreme temperatures and the synoptic environment at the times of record temperatures because of the availability of routine analyses. In addition, it allows the investigation of whether the number of extreme warm and cold days has changed since the stations were established.

Most of the stations we consider are located in the Antarctic coastal region; however, there are two long records from the interior plateau from Amundsen–Scott station at the South

Pole and Vostok station. We have not used the measurements made by AWSs since these systems are unattended for long periods and there are questions regarding the accuracy of the temperature observations in extreme conditions.

Quality control of the observations is extremely important in assessing extreme events, so this topic is discussed in section 2, along with the means by which we determined the thresholds for extreme conditions. Section 3 examines the frequency distributions of temperatures from the stations and the factors that influence the shape of the distributions. The highest and lowest temperatures recorded at the stations are discussed in section 4, along with the synoptic environments in which these occurred. The variability and trends in the occurrence of extreme warm and cold days over the full length of the records are considered in section 5. Conclusions are presented in section 6.

## 2. Data and methods

We use the synoptic observations of surface temperature made as part of the routine meteorological observing programs carried out at the stations up to the end of 2019. In the early parts of the records the measurements were made manually by observers at the main synoptic hours, with the data being collected every 3 or 6 h, or more infrequently depending on the availability of staff. Gradually, there was a transition to the automated collection of data, which allowed more frequent observations to be obtained, with hourly or more frequent data often being archived. The observations collected were brought together as part of the Scientific Committee on Antarctic Research (SCAR) Reference Antarctic Data for Environmental Research (READER) project (Turner et al. 2004), with the data being obtained from the operators of the national Antarctic programs. The data were subject to a rigorous quality control procedure (see Turner et al. 2004) and the computed monthly mean values up to 2015 form the basis of the online SCAR READER database (<https://legacy.bas.ac.uk/met/READER/>). Since 2015 we have used the reports from the station operators where possible but if these were not available, we used the synoptic reports distributed over the Global Telecommunications System. For these observations, we applied the same quality control procedure as applied to the earlier data. Briefly, this involved flagging erroneous observations by comparing the measurements with the climatological mean for the location and identifying outliers and unrealistic rapid changes in temperature. All record low and high temperatures were examined in detail by following the evolution of temperature and other meteorological parameters through the event and, for post-1979 records, examining the synoptic analyses from the ECMWF interim reanalysis (ERA-Interim). Details of the background to specific extreme temperature events are provided in the text.

We have investigated extreme temperatures at 17 stations (the locations are listed in Table 1 and indicated in Fig. 1) that have long, year-round records and that are distributed fairly evenly around the Antarctic coastline. Many of the records start around the time of the International Geophysical Year (IGY) in the late 1950s, with the shortest record examined being from Neumayer station, which starts in January 1981. We have not merged any records from nearby stations, but there have inevitably been small changes in the locations of some

TABLE 1. Stations considered in this study. Note that meteorological observations were first collected at Orcadas in 1904 but have only been digitized for the period since January 1956.

Station	Latitude	Longitude	Elevation (m)	Data period
Orcadas	60.73°S	44.73°W	6	Jan 1956–Dec 2019
Bellingshausen	62.18°S	58.95°W	16	Mar 1968–Dec 2019
Esperanza	63.40°S	57.00°W	13	Jan 1957–Dec 2019
Marambio	64.24°S	56.63°W	198	Jan 1971–Dec 2019
Vernadsky	65.25°S	64.25°W	11	Jan 1947–Dec 2019
Casey	66.28°S	110.53°E	41	Feb 1969–Dec 2019
Mirny	66.56°S	93.00°E	30	Feb 1956–Dec 2019
Dumont d'Urville	66.67°S	140.00°E	43	Apr 1956–Dec 2019
Rothera	67.57°S	68.13°W	16	Mar 1976–Dec 2019
Mawson	67.60°S	62.87°E	16	Feb 1954–Dec 2019
Molodezhnaya	67.67°S	45.83°E	40	Mar 1963–Jun 1999, Jan 2010–Dec 2019
Davis	68.58°S	77.97°E	13	Feb 1957–Dec 2019
Syowa	69.00°S	39.58°E	21	Feb 1957–Dec 2019
Neumayer	70.65°S	8.4°W	50	Jan 1981–Dec 2019
Novolazarevskaya	70.77°S	11.81°E	99	Feb 1961–Dec 2019
Vostok	78.46°S	106.84°E	3488	Jan 1958–Dec 2019
Amundsen–Scott	90.00°S	—	2800	Jan 1957–Dec 2019

stations because of rebuilds and relocations (where available, details are provided in the metadata section of the READER website at <https://legacy.bas.ac.uk/met/READER/metadata/metadata.html>). However, these should not have had a major impact on temperatures at most stations in the way that some wind records have been affected by relocations. We have not used data from Halley station on the Brunt Ice Shelf on the eastern side of the Weddell Sea in this study as the station has been moved inland five times during its lifetime in order to maintain a safe distance from the ice edge. This change in distance from the relatively warm ocean has affected the homogeneity of the temperature series, with at least one large jump in the record and other smaller changes. The station moves will also have affected the record of extreme temperatures at the station.

Making instrumental measurements at any location presents challenges, especially during extreme conditions, and great care needs to be exercised regarding the instruments used, the shielding of sensors, and the selection of a location for the instrument screen. In the Antarctic, most operators use a standard meteorological screen, which is located at a suitable site close to the main station. Such instruments provide satisfactory data under most conditions. However, it has been shown that in the Antarctic summer during periods of low wind speed and clear skies, temperatures measured in a standard screen can have a positive bias (Burton 2014; Genthon et al. 2011). Scatter diagrams of high temperatures against wind speed do show that a number of the record high temperatures reported in the station data occurred when the wind speed was very low. We have therefore provided two record high temperatures for each station—one being the highest temperature recorded regardless of wind speed, and the second for the highest temperature measured when the wind speed was 5 knots ( $1 \text{ kt} \approx 0.51 \text{ m s}^{-1}$ ) or greater.

Although some synoptic charts for high southern latitudes were drawn manually around the time of the IGY, there were very few observations over the ocean, and it is felt that the fields are not of high value in the analyses of the broadscale synoptic environment. We have therefore only considered the synoptic

situation in which extreme temperatures occurred for the period from 1979 as the reanalysis fields are well constrained by satellite data from this date onward. For this we used the fields from the ERA-Interim (Dee et al. 2011), which have a grid spacing of  $\sim 70 \text{ km}$ . A number of studies have conducted intercomparisons of the various reanalysis datasets and concluded that the ERA-Interim data are the best for depicting recent Antarctic climate (Bracegirdle and Marshall 2012).

There are many earlier studies that have examined changes in the daily maximum and minimum temperature either globally or for a particular region (e.g., European Academies Science Advisory Council 2013). However, as noted by Wei et al. (2019), such data are not readily available in digital form prior to 2000 for many of the Antarctic stations and where data have been digitized they do not cover the full length of the records. We have therefore elected to examine variability and change in the daily mean temperature, which we have calculated from the 0000, 0600, 1200, and 1800 UTC observations. The daily mean temperature has been used in many glaciological investigations where there is a requirement for data on positive degree-days (Barrand et al. 2013). Here we only computed a daily mean temperature if all four of the main 6-hourly synoptic observations were available. To identify the thresholds for extreme cold and warm days we have used the 5th and 95th percentiles of the temperature distribution, a method that has been used in many earlier investigations of extreme temperatures [see references in IPCC (2012)]. As the temperature records from the stations are of different length, we have determined the 5th and 95th percentiles for each station using temperatures for the 30-yr period 1980–2009 and then applied them over the full length of the records. Since the number of days in each year with valid data is variable, we show the percentage of days with extreme high and low temperatures rather than the actual number of days. We only compute the percentage of days with extreme temperatures if there are at least 90% of daily mean temperatures available in a year.

We calculated the trend in the percentage of days each year that had extreme temperatures using ordinary least squares

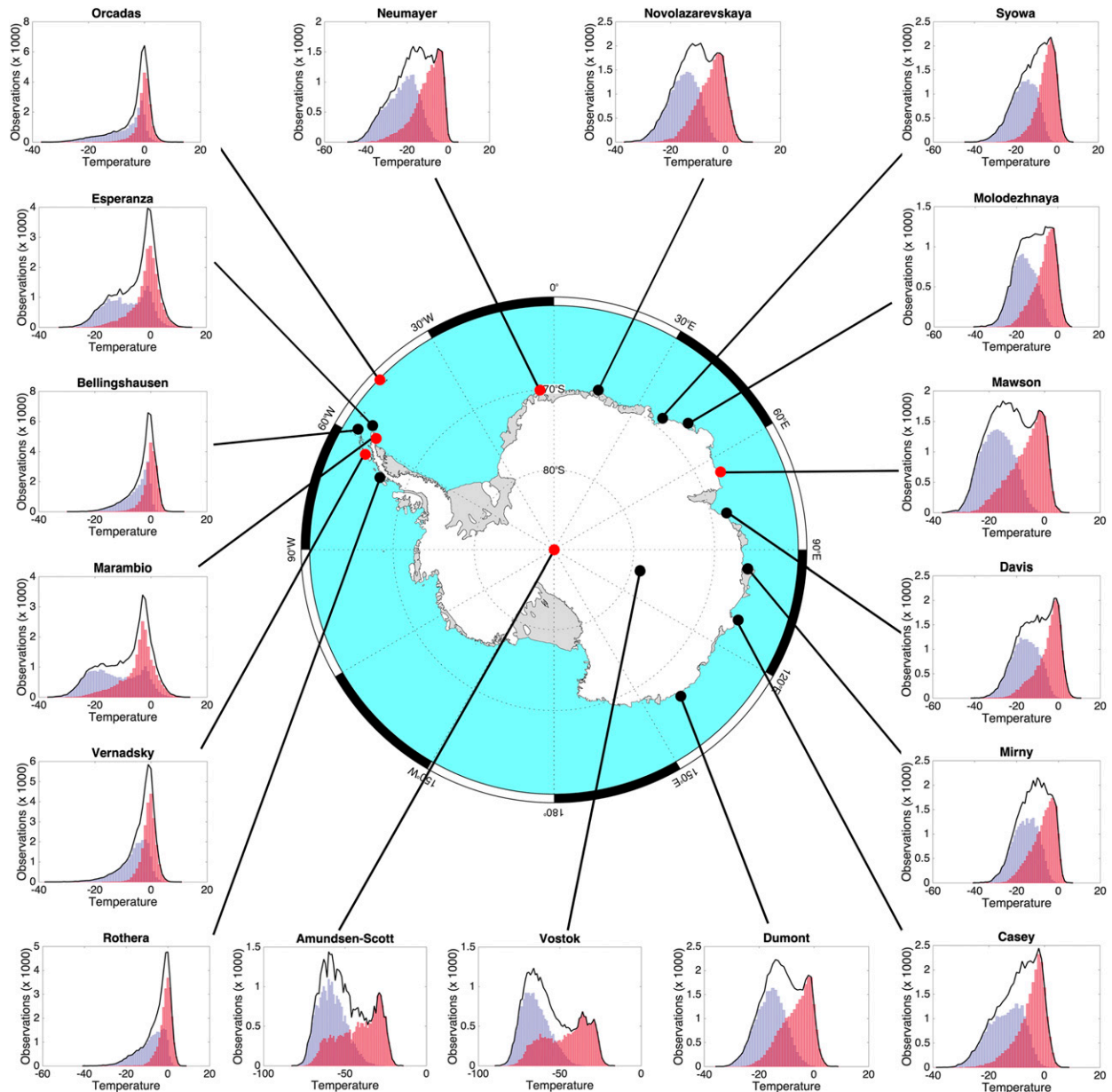


FIG. 1. Histograms of all 6-hourly temperature observations for the period 1980–2009 for the extended summer half year (November–April; light red) and the extended winter half year (May–October; blue). The overlap between the summer and winter histograms is indicated by dark red. The distribution of temperatures for the whole year are indicated by the black line. The figure also indicates the locations of the stations considered in this study with the red dots identifying the six stations considered in detail.

regression techniques, while using the nonparametric Mann–Kendall test to calculate trend significance (Alexander and Arblaster 2009). This test is widely used for evaluating the presence of monotonic trends and makes no assumption for normality, only that the data are temporally independent, so is appropriate for the extreme temperature data.

To investigate the relationships between the percentage of warm and cold extremes, and the major modes of climate variability we have used the index of the southern annular mode (SAM) developed by Marshall (2003) (<http://www.nerc-bas.ac.uk/>

[icd/gjma/sam.html](http://icd/gjma/sam.html)) and the Climate Prediction Centre Niño-3.4 seasonal temperature anomalies (<http://www.cpc.ncep.noaa.gov/data/indices/>). The percentage of warm and cold extremes each year has respectively been correlated with the summer and winter SAM index and Niño-3.4 temperature anomaly.

### 3. The temperature distributions at the stations

We first examine the frequency distributions of temperatures via histograms of all the 6-hourly synoptic observations



from the stations over the period 1980–2009 (Fig. 1). Data are presented for the extended summer half year (November–April), the extended winter half year (May–October), and the year as a whole. We will focus particularly on data from six stations covering the broad climatic regions across Antarctica. These are Orcadas at a maritime Antarctic island location, Marambio and Vernadsky (formerly Faraday) on the eastern and western sides of the Antarctic Peninsula, respectively, Neumayer on the coast of the eastern Weddell Sea, Mawson on the coast of East Antarctica, and Amundsen–Scott on the high interior plateau.

All the non-plateau stations have a negatively skewed annual temperature distribution with a long cold tail. As discussed below, this is because the extreme high temperatures are associated with transient warm-advection events (e.g., Bozkurt et al. 2018; King et al. 2017). In contrast, the very cold temperatures are associated with periods of isolation from warmer air masses, when there is often extensive sea ice cover, and when the temperatures can drop to very low values over extended periods (Ding et al. 2020; Turner et al. 2013; Turner et al. 2009). The extended summer distributions of the coastal East Antarctic stations have a more negatively skewed distribution than that for the extended winter. This is likely a result of the extended summer period including both the months when there are periods of 24 h of sunlight, and times when there is a period of darkness with lower temperatures.

For stations with a strong maritime influence, the annual temperature distributions have a single sharp peak close to freezing point as a result of the cold ocean temperatures that are found throughout much of the year. This is the case with Orcadas (Zazulie et al. 2010), which is the most northerly station examined (Fig. 1).

Vernadsky and Bellingshausen on the western side of the Antarctic Peninsula both have similar temperature distributions to Orcadas, reflecting the frequency of ice-free conditions at these locations (Turner et al. 2013). In the extended summer, there is little sea ice near Vernadsky (Parkinson 2014) and the strong maritime influence is reflected in the high proportion of temperatures close to the freezing point (Fig. 1). However, Rothera, in the more southerly part of the western Antarctic Peninsula, has a slightly broader annual temperature distribution because of the greater frequency of sea ice close to the station (Comiso and Nishio 2008).

A bimodal structure in the temperature distribution is apparent in the annual data from a number of stations, especially at more southerly latitudes. At Marambio (Fig. 1) it arises because of the ice-free conditions over the extended summer giving a sharp peak, coupled with a broader distribution in winter when there is more extensive and variable sea ice cover (Zwally et al. 2002). The two winter peaks correspond broadly to the frequent cold barrier winds from the south (King and Turner 1997) and westerlies crossing the Antarctic Peninsula, many of which are warmed by the foehn effect (Elvidge et al. 2016). A similar annual temperature distribution is found at Esperanza, although the winter cold peak is slightly less pronounced.

The extended winter distribution of temperatures at Vernadsky is broader than in the extended summer, reflecting the highly variable nature of sea ice and atmospheric circulation at this time

of year. Sea ice is particularly variable in the middle of winter when a polynya-like area of open water is found close to the station in some years (Turner et al. 2013). With open water near Vernadsky and air masses arriving from the north, midwinter temperatures can be several degrees above freezing (Turner et al. 2019b).

There are large differences in the shape of the annual temperature distribution for stations around the coast of East Antarctica. These vary from a single peak (Syowa) to a broad, flat distribution of temperature in the middle of the range (Molodezhnaya) to a clear bimodal structure (Dumont d'Urville). The distributions for the extended winter 6 months (Fig. 1, blue distributions) are quite similar for the majority of the stations, with a single peak in the distribution, although the kurtosis (sharpness of the peak) varies. The exception is Casey, which has a more bimodal winter temperature distribution, with the main peak at  $-10^{\circ}\text{C}$  and a secondary peak close to  $-18^{\circ}\text{C}$ . This form of distribution is most pronounced in May and September when the circumpolar trough is farther south and there is a minimum in the mean sea level pressure (MSLP) field off the station (van den Broeke 1998). The peak in the distribution at  $-10^{\circ}\text{C}$  is associated with the many cyclones that are found just off the coast in the area (Jones and Simmonds 1993), which bring relatively warm air from the north to the station. The peak at  $-18^{\circ}\text{C}$  is indicative of occasions when there are few depressions off the coast and low wind speeds that preserve the surface temperature inversion and lead to lower temperatures—the mean 10-m wind speed for occasions when surface temperature is in the range  $-17.0^{\circ}$  to  $-19.0^{\circ}\text{C}$  is  $4.1\text{ m s}^{-1}$ , compared to  $9.6\text{ m s}^{-1}$  for temperatures of  $-9.0^{\circ}$  to  $-11.0^{\circ}\text{C}$ . The differences in the winter temperature distributions are strongly influenced by the different wind regimes at the stations associated with local and broadscale factors.

The temperature distributions for the extended summer 6 months are mostly characterized by a single peak  $1^{\circ}\text{C}$  below freezing point because of the extensive areas of open water just north of the stations during this half year. But as with the distributions for the extended winter, the kurtosis varies. Syowa has a very narrow peak and a kurtosis of 4.13. In contrast, the distribution for Mawson has a broad tail of low temperatures (the kurtosis is 2.78) because of the high frequency of cold, katabatic winds, even during the summer half year.

On the Antarctic plateau the two stations with long records both have annual temperature distributions with a marked bimodal form, with the cold peak being more pronounced than the warm. The mean annual cycle of temperature at both stations has a clear signal of the coreless winter with an extended winter of low temperatures and a short, relatively warm summer (Thompson et al. 1970). Because of the length of the coreless winter (approximately March to October), the 6-month extended summer period we examine here (November to April) includes months of low temperatures, so that the extended summer temperature distributions for the two stations have a bimodal distribution, which is slightly more pronounced at Vostok.

#### 4. The extreme temperatures

We consider the record high and low temperatures recorded in the station synoptic observations (Table 2) and examine the conditions that led to such extreme conditions. Composite

TABLE 2. The record high and low temperatures recorded at the stations up to the end of 2019.

Station	Maximum temperature and the time and date	Maximum temperature and the time and date with the wind speed 5 kt or stronger	Minimum temperature and the time and date
Orcadas	13.5°C (1800 UTC 23 Dec 1987)	13.5°C (1800 UTC 23 Dec 1987)	−38.9°C (0000 UTC 28 Jun 1972)
Bellingshausen	11.2°C (1200 UTC 29 Jan 1982)	11.2°C (1200 UTC 29 Jan 1982)	−28.5°C (0600 UTC 5 Aug 1991)
Esperanza	17.5°C (0900 UTC 24 Mar 2015) <sup>a</sup>	17.5°C (0900 UTC 24 Mar 2015)	−31.8°C (1200 and 1800 UTC 8 Jul 1975)
Marambio	17.1°C (2100 UTC 23 Mar 2015)	15.2°C (1800 UTC 4 Jan 1979) <sup>b</sup>	−36.8°C (2100 UTC 25 Jul 1994)
Vernadsky	10.9°C (0000 UTC 25 Jan 1985 and 0100 UTC 31 Dec 1988)	10.9°C (0000 UTC 25 Jan 1985)	−42.4°C (0300 UTC 10 Aug 1958)
Casey	8.4°C (0900 UTC 30 Jan 1991)	8.0°C (0000 UTC 12 Jan 1980)	−38.0°C (2100 UTC 17 Jul 1976 and 0900 UTC 18 Jul 1986)
Mirny	6.7°C (0600 UTC 2 Jan 1998)	6.0°C (0000 UTC 9 Jan 1960)	−39.5°C (0000 UTC 20 Aug 1956 and 0600 UTC 15 Aug 1982)
Dumont d'Urville	8.7°C (0600 UTC 2 Jan 2002)	8.6°C (1200 UTC 30 Dec 2001)	−35.2°C (0000 UTC 18 Jul 1976)
Rothera	8.7°C (2000 UTC 20 Jan 2003)	8.0°C (0600 UTC 8 Feb 1999)	−39.5°C (1200 UTC 12 Aug 1980)
Mawson	9.0°C (0900 UTC 9 Jan 1974)	9.0°C (0900 UTC 9 Jan 1974)	−35.3°C (0300 UTC 16 Jul 1985)
Molodezhnaya	7.8°C (1200 UTC 9 Dec 1967)	7.8°C (1200 UTC 9 Dec 1967)	−39.2°C (0600 UTC 31 Aug 1993)
Davis	13°C (0600 UTC 7 Jan 1974)	13°C (0600 UTC 7 Jan 1974)	−40.7°C (0000 UTC 27 Apr 1998)
Syowa	9.3°C (0900 UTC 15 Jan 1969)	8.1°C (1500 UTC 1 Dec 1997)	−44.1°C (0200 UTC 4 Sep 1982)
Neumayer	4.4°C (0600 UTC 28 Mar 1991)	4.4°C (0600 UTC 28 Mar 1991)	−49.8°C (0000 UTC 8 Jul 2010)
Novolazarevskaya	9.7°C (1200 UTC 3 Feb 1996)	9.7°C (1200 UTC 3 Feb 1996)	−38.8°C (1800 UTC 8 Aug 1965)
Vostok	−14.4°C (0600 UTC 6 Jan 1974)	−14.4°C (0600 UTC 6 Jan 1974)	−89.2°C (0300 UTC 21 Jul 1983)
Amundsen–Scott	−12.3°C (1000 UTC 25 Dec 2011)	−12.3°C (1000 UTC 25 Dec 2011)	−81.7°C (0000 UTC 23 Jun 1982)

<sup>a</sup> A measurement of 18.3°C on 6 February 2020 has yet to be verified.

<sup>b</sup> Note that a temperature of 15.6°C was reported at 1800 UTC 6 February 2020.

anomalies in the MSLP (upper-air geopotential height fields for Amundsen–Scott) are presented for the days when the temperatures were beyond the thresholds listed in Table 3 during the post-1979 period.

Extreme high temperatures clearly occur during the extended austral summer, with most having been recorded in January, although the highest temperatures at Neumayer, Marambio, and Esperanza were all observed in March. High temperatures not linked to foehn dynamics are unlikely before December because of the extensive sea ice that influences temperatures at many stations. While there is a general north–south decrease in the record high temperatures that have been observed, Orcadas has not recorded a temperature as high as Esperanza and Marambio since air masses arriving at the station are not warmed to such an extent by the foehn effect as occurs at the stations in the northeastern part of the Antarctic Peninsula. The exact location of a station in relation to the local orography is extremely important in determining whether it experiences foehn winds, as evidenced by the much higher temperatures that have been recorded at Signy compared to the nearby Orcadas station.

Extreme low temperatures are invariably recorded during the extended winter season, with most occurring in July and August, although some were recorded in June and September. Conditions conducive to very low temperatures are isolation from relatively mild midlatitude air masses for extended periods and extensive sea ice cover in the vicinity of the station to limit the flux of heat and moisture from the ocean. Such conditions are found along the eastern side of the Weddell Sea, so that Neumayer has recorded extreme low temperatures below anything observed at the stations around the coast of East Antarctica.

In the following we examine the conditions that led to extreme temperatures at the six stations representative of different climatological zones within the Antarctic.

#### a. Orcadas

Orcadas, in the maritime Antarctic South Orkney Islands, has a climate that is strongly influenced by the many eastward moving storms over the Southern Ocean, along with cold air masses arriving from the cold, sea ice-covered Weddell Sea. The highest temperatures at the station have been associated with strong westerly flow between an area of high pressure over the South Atlantic and low pressure in the Weddell Sea (Fig. 2a). In this situation, the foehn effect increases the temperature as the air passes over the high orography of Coronation Island to the west of the station [e.g., see King et al. (2017) for a detailed investigation of a foehn wind affecting conditions on nearby Signy Island]. Low MSLP in the Bellingshausen Sea is associated with La Niña conditions in the tropical Pacific Ocean so the number of warm events at Orcadas has an anticorrelation of  $-0.3$  ( $p < 0.05$ ) with the Niño-3.4 index. The highest temperature recorded was 13.5°C at 1800 UTC 23 December 1987, with the temperature increasing from around 0°C to this record level in 12 h before decreasing to 2°C 12 h later. This short, rapid incursion of warm air, which was not observed at the nearby Signy station (Signy is not directly in the lee of Coronation Island during westerly winds), is characteristic of other very high temperature events occurring at the station.

The presence or absence of sea ice is particularly important in dictating the temperatures at the more northerly stations, as extensive sea ice limits the flux of heat from the ocean. At

TABLE 3. The upper and lower thresholds for extreme daily mean temperatures for the 17 stations based on the 5th and 95th percentiles determined from the daily mean temperature (mean of the temperatures at the four main reporting hours) for 1980–2009. We also include the range of months over which the extremes occurred in the period 1980–2009.

Station	Upper threshold	Range of months for upper extremes	Lower threshold	Range of months for lower extremes
Orcadas	2.5°C	January–December	−17.3°C	May–October
Bellingshausen	2.7°C	November–April	−11.3°C	April–October
Esperanza	3.7°C	January–December	−18.0°C	April–October
Marambio	2.2°C	January–December	−23.4°C	April–October
Vernadsky	2.3°C	August–June	−12.8°C	May–November
Casey	0.6°C	November–March, June, August	−21.9°C	March–October
Mirny	−0.9°C	November–March	−23.3°C	April–October
Dumont d'Urville	−0.1°C	November–March	−22.1°C	April–October
Rothera	2.3°C	October–June	−17.3°C	April–October
Mawson	0.7°C	November–February	−24.0°C	April–October
Molodezhnaya	−0.1°C	November–May	−23.5°C	April–October
Davis	1.5°C	November–April	−24.2°C	April–October
Syowa	0.1°C	November–March, May	−24.4°C	April–October
Neumayer	−2.7°C	November–April	−32.9°C	April–October
Novolazarevskaya	0.7°C	November–February	−22.3°C	April–October
Vostok	−30.0°C	November–February	−74.7°C	April–September
Amundsen–Scott	−25.9°C	November–February	−68.3°C	March–October

Orcadas the ice extent around the islands is highly variable in winter. This is reflected in the midwinter temperature distribution (not shown), which has peaks just below freezing and around  $-15^{\circ}\text{C}$ , corresponding to ice-free and ice-covered conditions, respectively. The lowest temperatures were associated with positive sea ice extent anomalies, with the ice extending northward from the Weddell Sea to the latitude of the South Orkney Islands. The mean MSLP anomalies for the occasions with the lowest temperatures at Orcadas (Fig. 3a) has a negative pressure anomaly to the east of the islands and positive anomaly over the Antarctic Peninsula. This pattern favors a strong southerly flow of cold air out of the Weddell Sea, in addition to advecting sea ice toward the region.

### b. The eastern Antarctic Peninsula

Temperatures on the eastern side of the Antarctic Peninsula are strongly influenced by the high orography to the west, with the extreme high temperatures associated with strong westerly winds. The mean MSLP anomaly for the highest 5% of temperatures at Marambio (Fig. 2b) is negative in the region of the Amundsen Sea low, with a positive anomaly over the southwestern Atlantic/Falkland Islands, implying that the belt of strong westerlies is displaced toward the south. This results in relatively warm air masses being further warmed by the foehn effect as they pass over the peninsula before arriving at the stations (Cape et al. 2015; Elvidge et al. 2016; Marshall et al. 2006). The highest temperature observed at Marambio was  $17.1^{\circ}\text{C}$  at 2100 UTC 23 March 2015, during a period of strong westerly winds involving warm air from the South Pacific. However, at the time of the record temperature, the wind speed had dropped to only 1 kt, so the temperature may have been higher because of enhancement through strong solar radiation onto the instrument enclosure. The highest temperature recorded at the station with a wind speed of more than 5 kt was  $15.2^{\circ}\text{C}$  at 1800 UTC 4 January 1979 during another strong westerly wind event involving air from the South Pacific. The period of strong westerlies over 23–24 March 2015 also gave

Esperanza its highest verified temperature of  $17.5^{\circ}\text{C}$ , which has been described in detail by Skansi et al. (2017).

It is surprising that temperatures as high as  $10.3^{\circ}\text{C}$  (at 0000 UTC 15 July 2010) have been recorded at Marambio in midwinter; however, Kirchgassner et al. (2019) showed that the temperatures on the eastern side of the Antarctic Peninsula during foehn events show little variability over the year. The synoptic environment when such high winter temperatures occur consists of a warm ridge extending southward from southern South America toward the Antarctic Peninsula, which brings warm South Pacific air over the eastern Bellingshausen Sea. The air then crosses the Antarctic Peninsula as a strong northwesterly with temperatures increased by the foehn effect.

Generally, the lowest temperatures on the eastern side of the Antarctic Peninsula are associated with a south to southeasterly airflow from the cold Weddell Sea when there is low pressure over the northwestern Weddell Sea (Fig. 3b). Under these conditions, there is greater sea ice advection than normal toward the northwest Weddell Sea, limiting the flux of heat from the ocean. The number of cold events is significantly anticorrelated ( $-0.34$ ,  $p < 0.05$ ) with the SAM index as weaker westerly winds are associated with more meridional flow out of the Weddell Sea. The lowest temperature recorded at Marambio ( $-36.8^{\circ}\text{C}$ , at 2100 UTC 25 July 1994) occurred toward the end of 6 days of decreasing temperature as high pressure built across the region from an anticyclone over the Bellingshausen Sea at the same time as a very deep low formed over the northeast Weddell Sea. In the marked MSLP gradient across the Weddell Sea very cold air was drawn toward the northwest Weddell Sea with the ERA-Interim reanalysis indicating that surface temperatures of  $< -35^{\circ}\text{C}$  occurred across a large part of the Weddell Sea.

### c. The western Antarctic Peninsula

The Antarctic Peninsula extends northward from the main body of the Antarctic and the temperatures at the stations are strongly influenced by synoptic-scale weather systems within

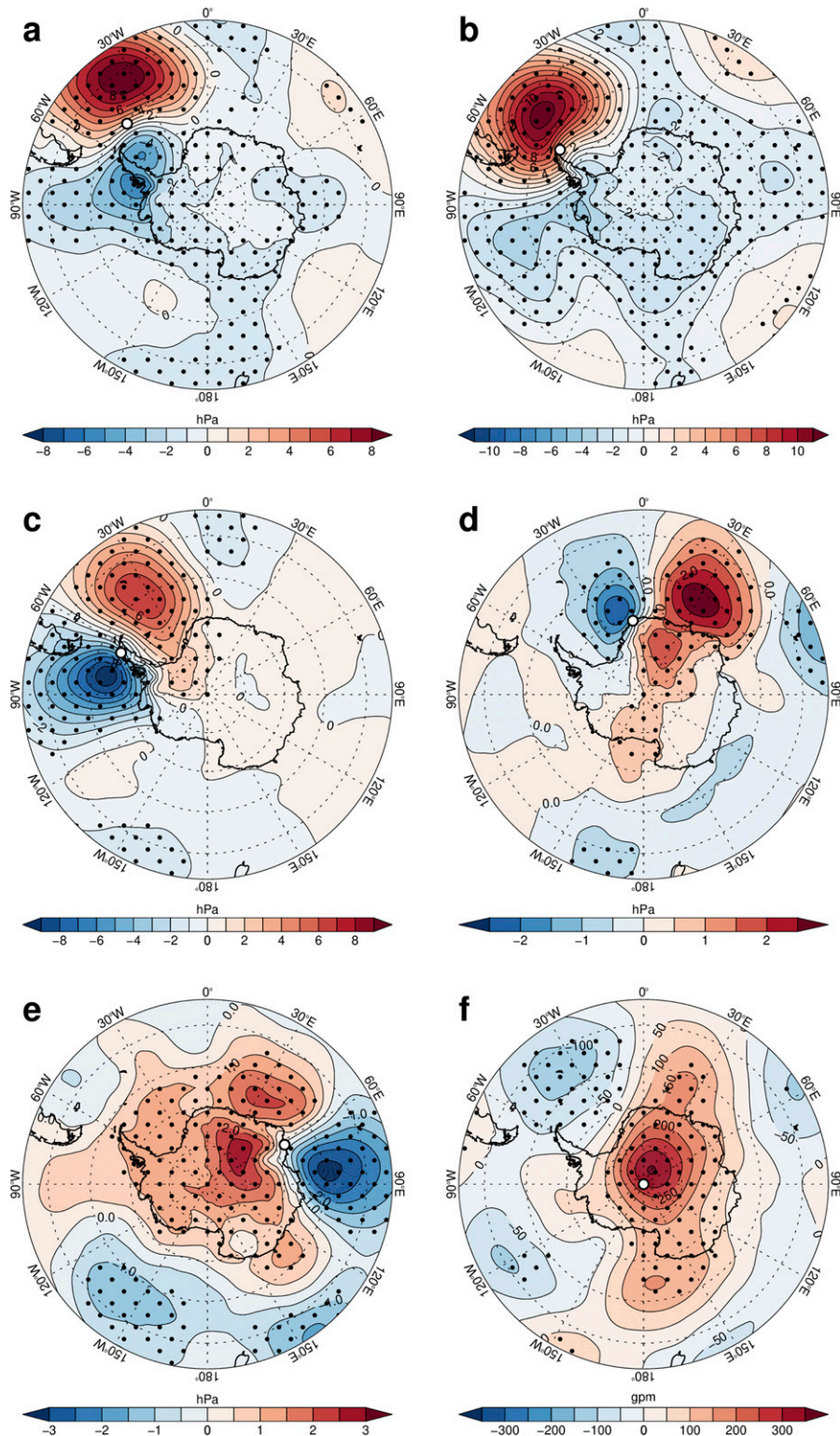


FIG. 2. The composite MSLP (500-hPa geopotential height for Amundsen–Scott) anomalies for the days during 1979–2019 when the temperatures at the stations were above the high temperature thresholds listed in Table 3, shown for (a) Orcadas, (b) Marambio, (c) Vernadsky, (d) Neumayer, (e) Mawson, and (f) Amundsen–Scott. The base period for the anomalies was the 31-day centered running mean (excluding the central day itself). The stippling indicates where the anomalies are statistically significant at  $p < 0.05$ . The location of each station is shown by a white dot.



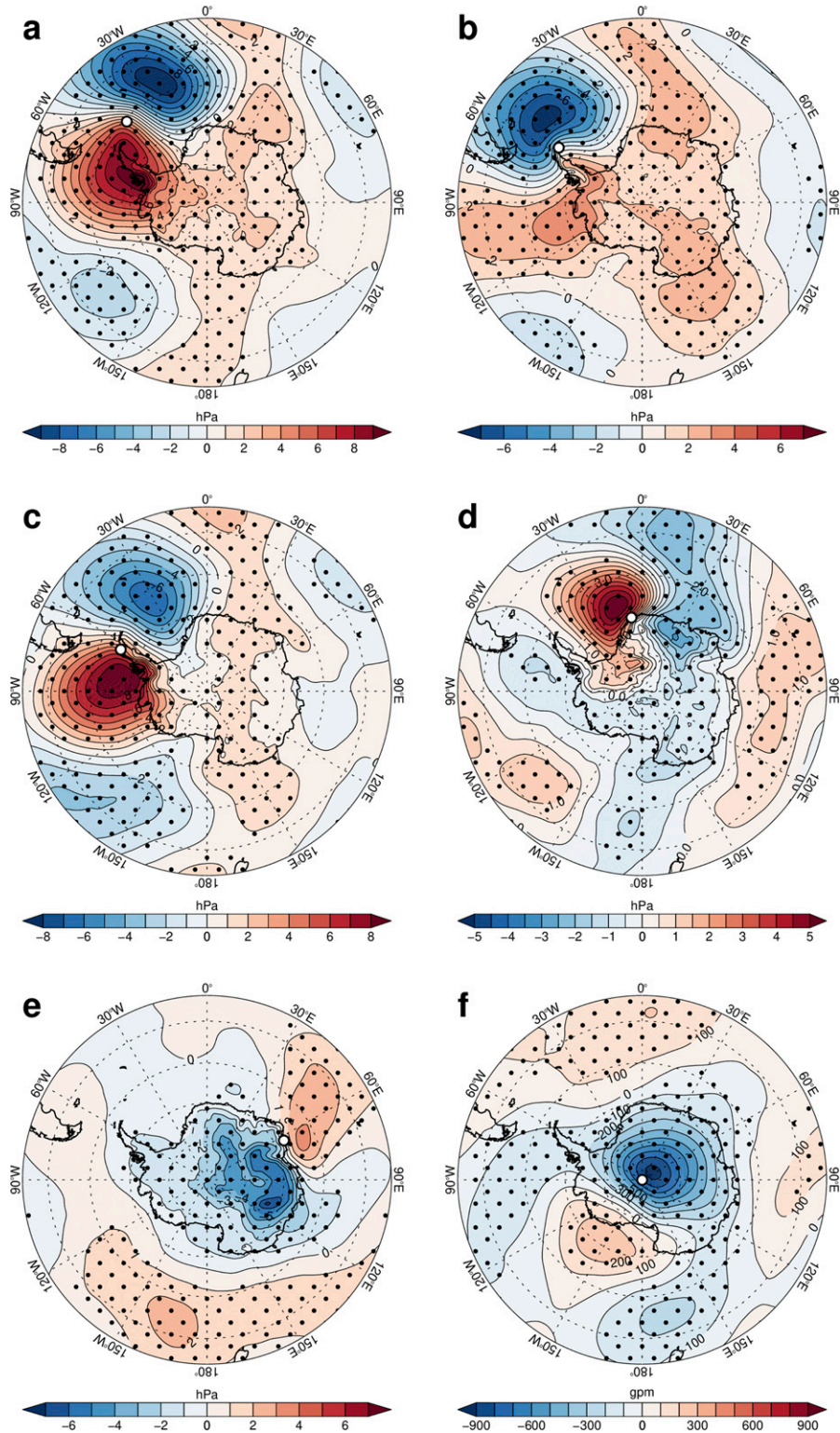


FIG. 3. As in Fig. 2, but for occasions when the temperatures were below the cold temperature threshold.

the climatological circumpolar trough that extends across 60°–70°S. The highest temperatures recorded at Vernadsky have been associated with large negative MSLP anomalies over the Bellingshausen Sea (Fig. 2c), with the lows in this area advecting warm air masses down the peninsula. Several factors are important in determining the temperatures at Vernadsky, including the location of the low in the Bellingshausen Sea, the pressure of the high in the Weddell Sea, and the origin of the air mass drawn toward the western side of the peninsula. In contrast, the lowest temperatures occurred with positive MSLP anomalies over the Bellingshausen Sea and negative anomalies in the Weddell Sea, giving cold-air advection over the region (Fig. 3c). The MSLP anomalies for high temperatures resemble a La Niña-like pattern (the anticorrelation between the number of warm events and the Niño-3.4 index is  $-0.34$ ,  $p < 0.01$ ), while the mean MSLP anomalies for low temperatures resemble an El Niño-like pattern. However, the warm extremes do not preferentially occur during La Niña conditions, nor the cold extremes during El Niño events. This highlights the different impacts of short-term, high-amplitude weather events and the lower-frequency preferential climate-mode type patterns that occur when averaged over El Niño and La Niña events.

The highest temperature in the Vernadsky record was 10.9°C, which was measured at 0000 UTC 25 January 1985 and 0100 UTC 31 December 1988. The 1985 record temperature occurred when a very deep depression with a central MSLP of <960 hPa was located over the southern Bellingshausen Sea giving strong warm-air advection down the western side of the peninsula. This was a relatively short-lived event, with temperatures increasing from 2°C to the record high and back to less than 4°C within 48 h.

High temperatures at Bellingshausen and Rothera are also often associated with deep depressions to the west of the peninsula that advect warm air from the north. This scenario gave the record high Bellingshausen temperature of 11.2°C at 1200 UTC 29 January 1982, although the advection of warm air was enhanced by a ridge of high pressure in the South Atlantic. However, the record high temperature at Rothera of 8.7°C at 2000 UTC 20 January 2003 occurred with high MSLP over the area, although the low wind speed of 4 kt coupled with cloud-free conditions may have resulted in the thermometer reading too high. In contrast, the temperature of 8.0°C at 0600 UTC 8 February 1999 occurred with a strong easterly flow across the peninsula, suggesting warming of the air as a result of the foehn effect.

Record low temperatures at stations on the western side of the Antarctic Peninsula are associated with strong southerly flow, bringing cold air masses across the region, often because of a couplet of relatively high pressure to the west of the peninsula and low pressure to the east (Fig. 3c). The Rothera record low temperature (1200 UTC 12 August 1980,  $-39.5^{\circ}\text{C}$ ) occurred with a very deep low pressure system in the Weddell Sea with a central pressure of <940 hPa, which contributed to the strong pressure gradient across the Antarctic Peninsula. The winter of 1980 was characterized by a large positive sea ice anomaly on the western side of the peninsula that was established as a result of the greater frequency of southerly flow. The record low temperature at Bellingshausen (0600 UTC 5 August 1991,  $-28.5^{\circ}\text{C}$ ) also occurred during a winter of positive sea ice anomaly over the Bellingshausen and Weddell Seas.

#### d. The eastern Weddell Sea

Neumayer experiences a climatological easterly wind as it is located on the southern side of the Circumpolar Trough. The highest temperatures recorded here generally occurred with lower pressure than normal over the northeastern Weddell Sea and high pressure in the Circumpolar Trough to the east Greenwich Meridian. This synoptic situation favors the advection of warm air masses toward the Antarctic coast down the Greenwich meridian (Fig. 2d). When Neumayer recorded its highest temperature of 4.4°C at 0600 UTC 28 March 1991 there was a complex area of low pressure to the northwest of the station that drew warm air from the north, but with only a ridge of high pressure to the east of the Greenwich meridian.

The lowest temperatures at Neumayer were recorded with a negative pressure anomaly over Dronning Maud Land and high MSLP in the Weddell Sea (Fig. 3d). This synoptic situation results in cold air masses arriving at the station from a generally southerly direction. The lowest temperature observed at the station was  $-49.8^{\circ}\text{C}$  at 0000 UTC 8 July 2010. The long-term mean July temperature at the station is  $-24.8^{\circ}\text{C}$ , and 2010 had the third coldest July in the record starting in 1982. The record low temperature occurred in the middle of a cold spell over the first 10 days of the month characterized by a trough of low pressure extending down Coats Land that advected cold air toward Neumayer from the south. The record low temperature on 8 July occurred as the wind speed dropped to 7 kt, enhancing the strength of the surface inversion.

#### e. East Antarctica

The composite MSLP anomaly field for the highest 5% of temperatures at Mawson has negative values close to 90°E and positive values near 30°E, suggesting that the highest temperatures at the station are associated with broadscale southerly flow off the continent (Fig. 2e). The warm events also occur with positive MSLP–upper-level height anomalies over the interior of the Antarctic, which is consistent with the significant anticorrelation ( $-0.53$ ,  $p < 0.01$ ) between the number of warm events each year and the SAM index. The positive MSLP anomaly inland of the station (also apparent in the surface pressure) will increase the strength of the coastal easterly wind, and also feed air from the interior down into the coastal zone. The plateau air has a high potential temperature and as it descends as a low-level flow will warm at the dry adiabatic lapse rate (DALR) and introduce air that is 5°–7°C warmer than that normally found in the coastal region. The warm events are also associated with a sharp trough to the east of Mawson, suggesting that air is advected up on to the plateau before its final descent to the station. If this air is of maritime origin its forced ascent to higher elevations inland of the coast will result in cooling at the saturated adiabatic lapse rate. Subsequent descent of dry air to the coast will warm the air mass at the DALR, giving a net warming before the air arrives at the station. The process is similar to that of the foehn effect, which is so important in giving high temperatures in the Antarctic Peninsula.

The highest temperature recorded at Mawson during the period for which we have reliable atmospheric analyses was 8.1°C at 1200 UTC 5 December 1989. The MSLP anomaly

during this event was very similar to that shown in Fig. 2e, with a deep low near 90°E and a sharp trough just to the east of Mawson. Back trajectories from Mawson indicate that the air responsible for the record high temperature originated on the Antarctic plateau and descended to the coastal region near 100°E, before being carried toward the station in the strong coastal easterlies. In addition, satellite imagery shows extensive cloud over the Amery Ice Shelf ahead of the relatively warm plateau air, suggesting an involvement of both maritime air aloft associated with the coastal depression and the near-surface air descending from the plateau.

While Fig. 2e shows the mean MSLP anomaly field for the highest 5% of temperatures at Mawson, examination of individual cases of warm events at the station shows some different scenarios associated with high temperatures. For example, the temperature of 7.3°C recorded at 0900 UTC 19 December 1982 occurred when there was a marked ridge to the west of the station that advected air inland close to 45°E, before it descended to Mawson along 60°E. Flow down from the interior is also a feature of high temperatures at Dumont d'Urville station, with forced ascent of air up onto the plateau and then descent down the glacial valleys. However, the highest temperatures recorded at some other stations around the coast of East Antarctica, such as Davis and Casey, are associated with warm air advected around a low north of the station and carried directly to the station in the strong easterly flow.

Low temperatures at Mawson are associated with relatively high MSLP to the north of the station and low pressure over the Antarctic interior (the correlation of the number of cold events with the SAM is 0.38,  $p < 0.01$ ), a situation that will weaken the coastal easterlies, with the airflow around the low drawing cold air from the interior (Fig. 3e). The relatively high pressure will promote generally cloud-free conditions and give greater cooling through emission of longwave radiation. However, the speed of the southerly wind must not be too strong or else the surface temperature inversion will break down.

The lowest temperature recorded at the station was  $-35.3^{\circ}\text{C}$  at 0300 UTC 16 July 1985. The synoptic situation when this record low temperature was recorded was rather different to that for many of the other very low temperatures. On this occasion a deep depression with a central pressure of  $<956$  hPa was present in the Antarctic coastal region close to 120°E and a marked trough extended to almost 80°S over the Amery Ice Shelf. This resulted in a southerly flow of cold air from the interior to the coastal region, although at the time of the lowest temperature the wind speed had dropped to just  $1\text{ m s}^{-1}$ .

#### f. The Antarctic Plateau

High temperatures at Amundsen–Scott station arise as a result of intrusions of warm air from the coastal region when the planetary waves are amplified over the continent (see Sinclair 1981). The mean 500-hPa geopotential height anomalies for the days with the highest 5% of temperatures at the station (Fig. 2f) has a positive anomaly close to the South Pole at 30°E. Warm air can arrive at the South Pole from any sector of the continent, but as suggested in Fig. 2f, most incursions of warm air arrive from close to the Greenwich meridian at a time when there is low pressure over the Weddell Sea (Clem et al. 2020). However, the highest temperature observed at the

station was  $-12.3^{\circ}\text{C}$  at 1000 UTC 25 December 2011, with the temperature being recorded during an intrusion of very warm air from the Bellingshausen Sea sector that lasted several days.

Very low temperatures at Amundsen–Scott are a result of isolation from relatively warm air masses originating in lower latitudes, particularly when the SAM is positive (the correlation of the number of warm events with the SAM index is 0.37,  $p < 0.01$ ). The mean 500-hPa geopotential height anomaly for the coldest days (Fig. 3f) has small-amplitude planetary waves and a center of negative anomaly located close to the station. This is broadly the same scenario as occurred during the record low temperature recorded at Vostok station in 1989 (Turner et al. 2009).

The lowest temperature at Amundsen–Scott station was  $-81.7^{\circ}\text{C}$  recorded at 0000 UTC 23 June 1982. During the period leading up to this event there was little thermal advection into the interior of the continent and the circulation at 500 hPa consisted of a circular flow that kept warm air masses from the interior of the Antarctic. However, this regime broke down within two days, with the temperature increasing rapidly to  $-53^{\circ}\text{C}$ .

## 5. Variability and change in the frequency of extreme daily mean temperatures

We have examined variability and change of extreme high and low temperatures via the number of daily mean temperatures that exceeded the 5th and 95th percentiles. The warm and cold threshold values (Table 3) were computed using all the daily mean values over 1980–2009. To take account of the variability in the number of valid daily mean temperatures between years, we consider the percentage of days each year with extreme warm or cold days.

The time series of the percentage of days that were classified as warm or cold for each year over the full length of the records for the six stations considered in detail are presented in Figs. 4 and 5. We only consider years when there were daily mean temperatures available for 90% of the days. In the following we examine the variability and change in the percentage of warm and cold extreme days for stations in the six regions discussed earlier.

### a. Orcadas

High temperatures at Orcadas occur with strong westerly winds, with the foehn effect increasing temperatures as the air passes over high orography. Over recent decades the strength of the westerlies has increased in summer, at least in part because of the ozone hole (Abram et al. 2014). This has shifted the SAM to being predominantly in its positive polarity (Marshall 2003). The positive trend in the percentage of warm days at Orcadas ( $0.60\%$  decade $^{-1}$ ,  $p < 0.01$ ) (Fig. 4a) is consistent with the westerly wind increases over recent decades. The largest increase in warm days was from the start of the record until the late 1990s, with a subsequent decrease. The percentage of days with cold conditions has not changed significantly since the start of the record.

### b. The eastern Antarctic Peninsula

Marambio has experienced a statistically significant increase ( $0.56\%$  decade $^{-1}$ ,  $p < 0.05$ ) in the percentage of extreme warm days over the record, which starts in the early 1970s. However, since the start of the twenty-first century the percentage of days



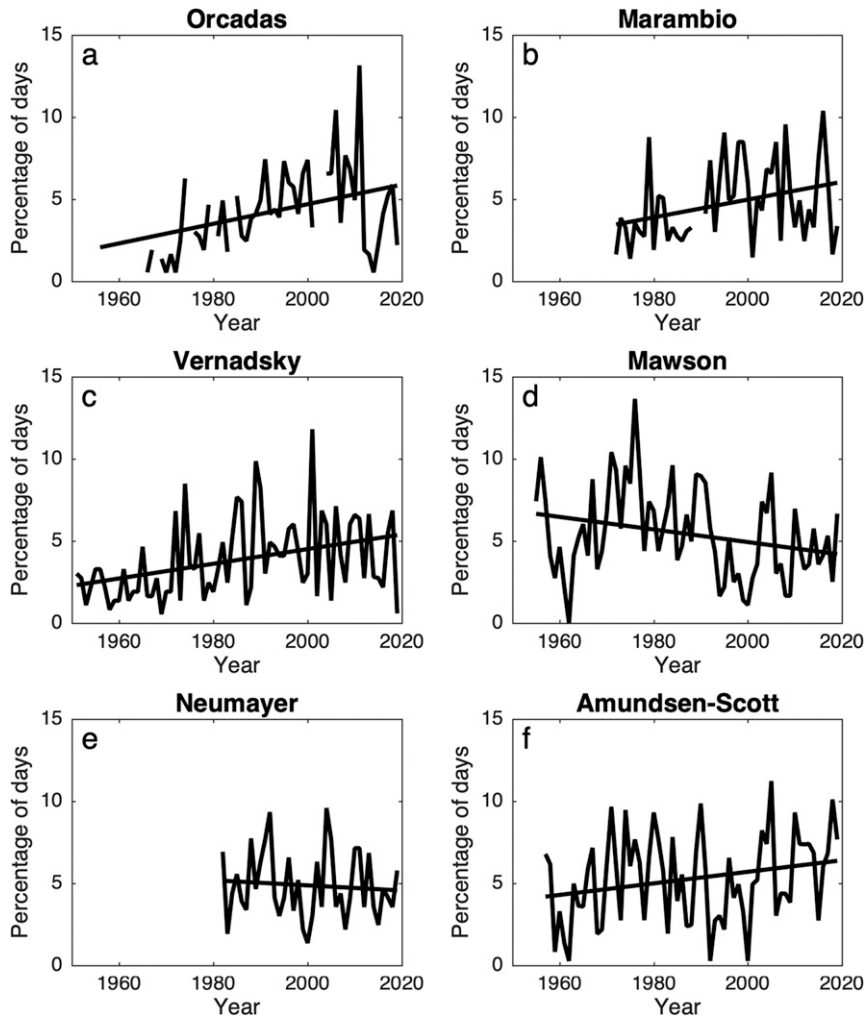


FIG. 4. Time series of the percentage of days each year with daily mean temperatures above the high temperature thresholds given in Table 3.

with extreme warm temperatures has remained constant or decreased slightly, consistent with the summer surface temperatures, which increased markedly until the late 1990s, but have then decreased since that time (Turner et al. 2016). At Marambio the number of cold days has decreased since the late 1970s at a rate of  $-0.23\%$  decade $^{-1}$ , although this trend was not significant.

#### c. The western Antarctic Peninsula

Bellingshausen and Vernadsky have both experienced an increase in the percentage of extreme warm days and decrease in cold days over the full length of their temperature records. The decrease in the percentage of cold days at Vernadsky ( $-1.67\%$  decade $^{-1}$ ,  $p < 0.05$ ) (Fig. 5c) was the largest decrease in cold days of any of the stations and is consistent with the large winter warming observed over the second half of the twentieth century and the loss of sea ice in midwinter (Turner et al. 2013). There was also a significant increase ( $0.45\%$  decade $^{-1}$ ,  $p < 0.01$ ) in the number of warm days, which was again most pronounced in the period up to 2000.

The annual percentage of extreme warm days at Vernadsky is rather variable as illustrated by the switch in the number of extremes between 2018 (6.9%) and 2019 (0.6%) (Fig. 4c). As would be expected, most of the warm days in 2018 occurred during the summer months, but extreme high temperatures also occurred in March, April, October, and November. The large number of warm days was a result of the greater number of deep storms to the west of the Antarctic Peninsula advecting warm air into the region.

The five stations examined from the Antarctic Peninsula region all experienced a statistically significant ( $p < 0.01$ ) increase in extreme high temperatures in the late-twentieth-century part of their records, although the number of extremes decreased in subsequent years.

#### d. The eastern Weddell Sea

Over the full length of the record Neumayer experienced a decrease in the number of extreme high temperatures and increase in low temperatures, although neither trend was statistically significant.



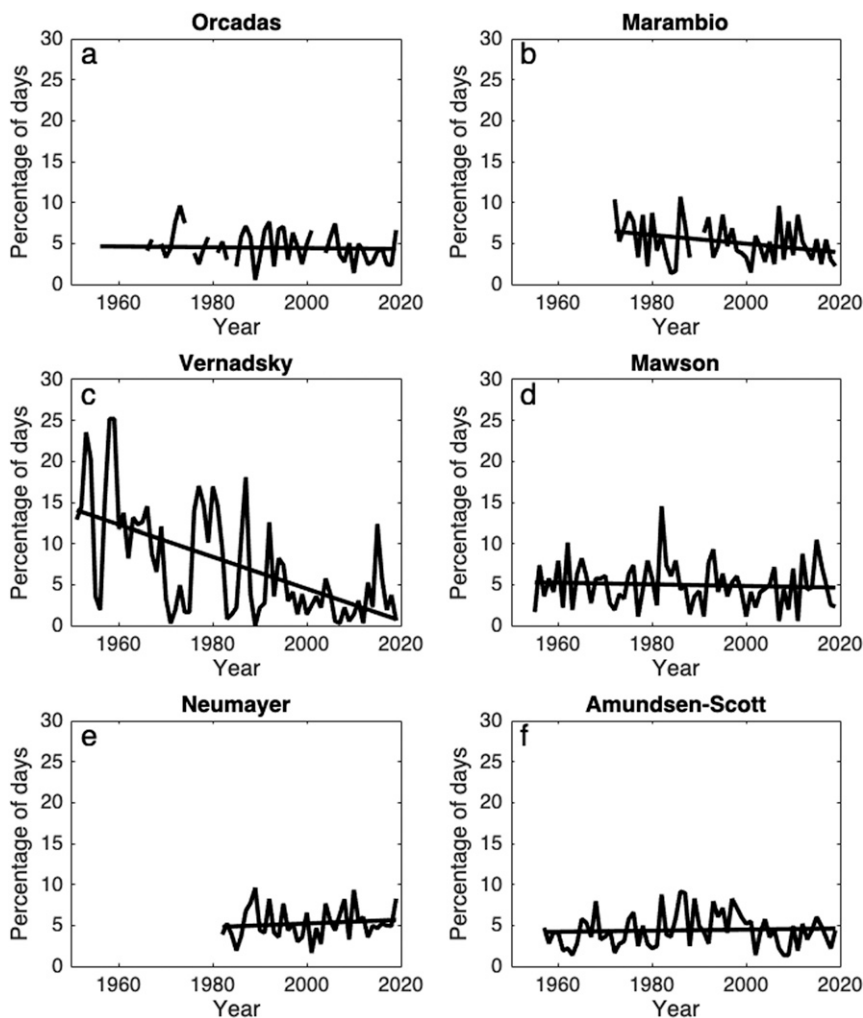


FIG. 5. As in Fig. 4, but showing the percentage of days each year with daily mean temperatures below the low temperature thresholds given in Table 3.

#### e. East Antarctica

Around the coast of East Antarctica there has been an overall small reduction in the number of extreme warm and cold days at many of the stations over the full length of the records (Table 4). The largest trends have been the decreases in the percentage of warm days at Casey ( $-0.71\%$  decade $^{-1}$ ,  $p < 0.05$ ), Mawson ( $-0.37\%$  decade $^{-1}$ ,  $p < 0.10$ ), and Molodzhnaya ( $-0.91\%$  decade $^{-1}$ ,  $p < 0.05$ ). These trends are consistent with the small decreases in summer temperatures at the stations, which has been linked to the loss of stratospheric ozone and the decrease in poleward heat flux. The largest decrease in cold days at the East Antarctic coastal stations has been at Novolazarevskaya ( $-0.42\%$  decade $^{-1}$ ,  $p < 0.05$ ), which was dominated by the reduction over the 1960s to the 1990s. There has been no significant trend in the SAM during the winter so the change must have occurred as a result of other factors.

#### f. The Antarctic Plateau

The two stations on the Antarctic Plateau have both experienced a significant positive trend in the percentage of

warm days over the records extending back to the late 1950s. The positive trend in the percentage of warm days at Vostok ( $0.57\%$  decade $^{-1}$ ,  $p < 0.01$ ) was the largest of any of the stations outside of the Antarctic Peninsula.

## 6. Conclusions

Our investigation of extreme temperatures in the Antarctic has highlighted the importance of flow over orography in creating the conditions that lead to record high temperatures. It has been well known for some time that the foehn effect plays an important part in establishing the conditions that give very high temperatures at some stations around the Antarctic Peninsula. However, it has not previously been reported that the highest temperatures at Mawson on the coast of East Antarctica occur when there is strong flow down the glacial valleys associated with a low to the east of a station and a ridge to the west. The air on the plateau inland of Mawson has a high potential temperature and can also be warmed through descent of air in a midtropospheric ridge over the area. However, air

TABLE 4. Decadal trends in the percentage of extreme warm and cold days over the full length of the records and for 1979–2019. The significance of the trends is indicated with asterisks: \*,  $p < 0.1$ ; \*\*,  $p < 0.05$ ; \*\*\*,  $p < 0.01$ .

Station	Warm (% decade <sup>-1</sup> ), full length	Cold (% decade <sup>-1</sup> ), full length	Warm (% decade <sup>-1</sup> ), 1979–2019	Cold (% decade <sup>-1</sup> ), 1979–2019
Orcadas	0.60***	-0.05	0.19	-0.29
Bellingshausen	0.22	-1.05***	-0.55**	-0.99
Esperanza	0.65***	-0.78***	0.31	-0.29
Marambio	0.54**	-0.53**	0.28	-0.23
Vernadsky	0.45***	-1.95***	-0.02	-1.67**
Casey	-0.71**	-0.19	-0.68	-0.14
Mirny	-0.22	-0.34*	-0.32	-0.33
Dumont d'Urville	0.07	-0.16	-0.42	-0.15
Rothera	-0.32	-1.04	-0.45	-0.95
Mawson	-0.37*	-0.10	-0.65*	-0.47
Molodezhnaya	-0.91**	-0.21	-1.25**	-0.61
Davis	0.05	0.13	-0.17	0.08
Syowa	-0.06	-0.26	-0.31	-0.05
Neumayer	-0.16	0.23	-0.16	0.23
Novolazarevskaya	0.12	-0.42**	-0.34	0.05
Vostok	0.57***	0.06*	0.29	-0.27
Amundsen–Scott	0.35*	0.02*	0.44	-0.48

can also be forced up to the plateau on the western side of a ridge in the coastal area before descent down the glacial valleys. Our study has also highlighted the importance of sea ice in leading to record low temperatures. At Orcadas and the stations on the Antarctic Peninsula southerly flow leads to northward advection of sea ice, which then limits the flux of heat from the relatively warm ocean.

Over recent decades there has been an increase in the number of extreme high temperatures observed over Earth as a whole (Alexander et al. 2006; Brown et al. 2008), with anthropogenic influences being strongly linked to this upward trend (Fischer and Knutti 2015). However, there are large regional variations in these trends, with some areas having experienced a decrease in the number of warm days (Alexander et al. 2006). Clearly regional factors are playing a part and natural climate variability will mask some of the anthropogenic influences on these small scales. While a number of these global studies into extreme temperatures have used data from the Antarctic stations to consider change on a global basis, none has examined the trends in extreme temperatures at specific Antarctic stations.

Overall, the trends in the frequency of warm and cold extreme temperatures across the Antarctic are similar to the trends seen in the mean temperatures at the stations. The most pronounced signals being a tendency toward higher temperatures/more extreme warm days over the Antarctic Peninsula and a small cooling/more extreme cold days around the coast of East Antarctica. This was particularly the case from the start of the records until the late 1990s with a reduction in these trends during the twenty-first century. This pattern of contrasting trends between the Antarctic Peninsula and the rest of the Antarctic is characteristic of the impact of the SAM on Antarctic temperatures (e.g., Marshall and Thompson 2016; Fogt and Marshall 2020) and has been seen in the ice core records as well as the station observations. During the second half of the twentieth century there was a positive trend in the SAM during summer (Marshall 2003), with the springtime loss of stratospheric ozone contributing to this change from the early 1980s. However,

since the start of the twenty-first century there has been little trend in the SAM and local variability in the atmospheric circulation has had a major effect on temperatures on the Antarctic Peninsula (Turner et al. 2016).

In situ observations, reanalysis datasets and ice-core climate records have shown that the atmospheric circulation around the Antarctic Peninsula is highly variable on interannual and decadal time scales (Connolley 1997). This makes it particularly difficult to detect a signal of the impact of increasing greenhouse gas concentrations. Whereas there is now strong evidence that the global increase in extreme high temperatures can be attributed to increasing greenhouse gases, local factors, such as the loss of stratospheric ozone and changes in the extent of sea ice, have been more important in driving the trends in extreme temperatures in the Antarctic over recent decades (Polvani et al. 2011; Turner et al. 2013).

During the twenty-first century we anticipate a recovery of the Antarctic ozone hole. However, if greenhouse gas concentrations continue to rise, we expect an increase in near-surface temperatures across the Antarctic of several degrees by the end of this century (Bracegirdle et al. 2008). With an overall shift of the temperature distributions to the right we can therefore expect an increase in the number of extreme high temperatures and decrease in low temperatures over this period. This potential change could be investigated using the output of global climate model experiments, where 6-hourly data would allow the construction of temperature distributions at various points over the twenty-first century. The anticipated temperature changes will have the greatest impact in the coastal areas of the continent and projections of the frequency of extreme events will aid investigations into ice shelf collapse and changes in the terrestrial biota.

*Acknowledgments.* This work forms part of the Polar Science for Planet Earth program of the British Antarctic Survey, Natural Environment Research Council. We are grateful to Dr. Matthew Lazzara, Antarctic Meteorological Research Center,

Space Science and Engineering Center, University of Wisconsin–Madison, USA, for providing satellite imagery of the Mawson area.

**Data availability statement.** The individual Antarctic station observations are available at [ftp://ftp.bas.ac.uk/ssbsrc/SCAR\\_EGOMA/SURFACE/](ftp://ftp.bas.ac.uk/ssbsrc/SCAR_EGOMA/SURFACE/). The ECMWF reanalysis fields can be found at <https://www.ecmwf.int/en/forecasts/datasets/reanalysis-datasets/era-interim>.

#### REFERENCES

- Abram, N. J., R. Mulvaney, F. Vimeux, S. J. Phipps, J. Turner, and M. H. England, 2014: Evolution of the Southern Annular Mode during the past millennium. *Nat. Climate Change*, **4**, 564–569, <https://doi.org/10.1038/nclimate2235>.
- Alexander, L. V., and J. Arblaster, 2009: Assessing trends in observed and modelled climate extremes over Australia in relation to future projections. *Int. J. Climatol.*, **29**, 417–435, <https://doi.org/10.1002/JOC.1730>.
- , and Coauthors, 2006: Global observed changes in daily climate extremes of temperature and precipitation. *J. Geophys. Res.*, **111**, D05109, <https://doi.org/10.1029/2005JD006290>.
- Alvarez, J. A., and B. J. Lieske, 1960: The Little America blizzard of May 1957. *Proc. Symp. on Antarctic Meteorology*, Melbourne, VIC, Australia, Australian Bureau of Meteorology, 115–127.
- Barrand, N. E., D. G. Vaughan, N. Steiner, M. Tedesco, P. Kuipers Munneke, M. R. van den Broeke, and J. S. Hosking, 2013: Trends in Antarctic Peninsula surface melting conditions from observations and regional climate modeling. *J. Geophys. Res. Earth Surf.*, **118**, 315–330, <https://doi.org/10.1029/2012JF002559>.
- Bozkurt, D., R. Rondanelli, J. C. Marin, and R. Garreaud, 2018: Foehn event triggered by an atmospheric river underlies record-setting temperature along continental Antarctica. *J. Geophys. Res. Atmos.*, **123**, 3871–3892, <https://doi.org/10.1002/2017JD027796>.
- Bracegirdle, T. J., and G. J. Marshall, 2012: The reliability of Antarctic tropospheric pressure and temperature in the latest global reanalyses. *J. Climate*, **25**, 7138–7146, <https://doi.org/10.1175/JCLI-D-11-00685.1>.
- , W. M. Connolley, and J. Turner, 2008: Antarctic climate change over the twenty first century. *J. Geophys. Res.*, **113**, D03103, <https://doi.org/10.1029/2007JD008933>.
- Brown, S. J., J. Caesar, and C. A. T. Ferro, 2008: Global changes in extreme daily temperature since 1950. *J. Geophys. Res.*, **113**, D05115, <https://doi.org/10.1029/2006JD008091>.
- Burton, B., 2014: Stevenson screen temperatures—An investigation. *Weather*, **69**, 156–160, <https://doi.org/10.1002/wea.2166>.
- Cape, M. R., M. Vernet, P. Skvarca, S. Marinsek, T. Scambos, and E. Domack, 2015: Foehn winds link climate-driven warming to ice shelf evolution in Antarctica. *J. Geophys. Res. Atmos.*, **120**, 11 037–11 057, <https://doi.org/10.1002/2015JD023465>.
- Cardil, A., D. M. Molina, and L. N. Kobziar, 2014: Extreme temperature days and their potential impacts on southern Europe. *Nat. Hazards Earth Syst. Sci.*, **14**, 3005–3014, <https://doi.org/10.5194/nhess-14-3005-2014>.
- Clem, K., R. L. Fogt, J. Turner, B. R. Lintner, G. J. Marshall, J. R. Miller, and J. A. Renwick, 2020: Record warming at the South Pole during the past three decades. *Nat. Climate Change*, **10**, 762–770, <https://doi.org/10.1038/s41558-020-0815-z>.
- Comiso, J. C., and F. Nishio, 2008: Trends in the sea ice cover using enhanced and compatible AMSR-E, SSM/I and SMMR data. *J. Geophys. Res.*, **113**, C02S07, <https://doi.org/10.1029/2007JC004257>.
- Connolley, W. M., 1997: Variability in annual mean circulation in southern high latitudes. *Climate Dyn.*, **13**, 745–756, <https://doi.org/10.1007/s003820050195>.
- Dee, D. P., and Coauthors, 2011: The ERA-Interim reanalysis: Configuration and performance of the data assimilation system. *Quart. J. Roy. Meteor. Soc.*, **137**, 553–597, <https://doi.org/10.1002/qj.828>.
- Ding, Y. F., X. Cheng, X. C. Li, M. Shokr, J. W. Yuan, Q. H. Yang, and F. M. Hui, 2020: Specific relationship between the surface air temperature and the area of the Terra Nova Bay Polynya, Antarctica. *Adv. Atmos. Sci.*, **37**, 532–544, <https://doi.org/10.1007/s00376-020-9146-2>.
- Elvidge, A. D., I. A. Renfrew, J. C. King, A. Orr, and T. A. Lachlan-Cope, 2016: Foehn warming distributions in nonlinear and linear flow regimes: A focus on the Antarctic Peninsula. *Quart. J. Roy. Meteor. Soc.*, **142**, 618–631, <https://doi.org/10.1002/qj.2489>.
- European Academies Science Advisory Council, 2013: Trends in extreme weather events in Europe: Implications for national and European Union adaptation strategies. EASAC Policy Rep. 22, 20 pp., [https://easac.eu/fileadmin/PDF\\_s/reports\\_statements/Easac\\_Report\\_Extreme\\_Weather\\_Events.pdf](https://easac.eu/fileadmin/PDF_s/reports_statements/Easac_Report_Extreme_Weather_Events.pdf).
- Fischer, E., and R. Knutti, 2015: Anthropogenic contribution to global occurrence of heavy-precipitation and high-temperature extremes. *Nat. Climate Change*, **5**, 560–564, <https://doi.org/10.1038/nclimate2617>.
- Fogt, R. L., and G. J. Marshall, 2020: The southern annular mode: Variability, trends, and climate impacts across the Southern Hemisphere. *Wiley Interdiscip. Rev.: Climate Change*, **11**, <https://doi.org/10.1002/wcc.652>.
- Genthon, C., D. Six, V. Favier, M. A. Lazzara, and L. M. Keller, 2011: Atmospheric temperature measurement biases on the Antarctic Plateau. *J. Atmos. Oceanic Technol.*, **28**, 1598–1605, <https://doi.org/10.1175/JTECH-D-11-00095.1>.
- IPCC, 2012: *Managing the Risks of Extreme Events and Disasters to Advance Climate Change Adaptation*. Cambridge University Press, 582 pp.
- Jones, D. A., and I. Simmonds, 1993: A climatology of Southern Hemisphere extratropical cyclones. *Climate Dyn.*, **9**, 131–145, <https://doi.org/10.1007/BF00209750>.
- King, J. C., and J. Turner, 1997: *Antarctic Meteorology and Climatology*. Cambridge University Press, 424 pp.
- , D. Bannister, J. S. Hosking, and S. R. Colwell, 2017: Causes of the Antarctic region record high temperature at Signy Island, 30th January 1982. *Atmos. Sci. Lett.*, **18**, 491–496, <https://doi.org/10.1002/asl.793>.
- Kirchgaessner, A., J. King, and A. Gadian, 2019: The representation of föhn events to the east of the Antarctic Peninsula in simulations by the Antarctic Mesoscale Prediction System. *J. Geophys. Res. Atmos.*, **124**, 13 663–13 679, <https://doi.org/10.1029/2019JD030637>.
- Marshall, G. J., 2003: Trends in the southern annular mode from observations and reanalyses. *J. Climate*, **16**, 4134–4143, [https://doi.org/10.1175/1520-0442\(2003\)016<4134:TTSAM>2.0.CO;2](https://doi.org/10.1175/1520-0442(2003)016<4134:TTSAM>2.0.CO;2).
- , and D. W. J. Thompson, 2016: The signatures of large-scale patterns of atmospheric variability in Antarctic surface temperatures. *J. Geophys. Res. Atmos.*, **121**, 3276–3289, <https://doi.org/10.1002/2015JD024665>.
- , A. Orr, N. P. M. van Lipzig, and J. C. King, 2006: The impact of a changing Southern Hemisphere annular mode on Antarctic Peninsula summer temperatures. *J. Climate*, **19**, 5388–5404, <https://doi.org/10.1175/JCLI3844.1>.
- Nicolas, J. P., and D. H. Bromwich, 2011: Climate of West Antarctica and influence of marine air intrusions. *J. Climate*, **24**, 49–67, <https://doi.org/10.1175/2010JCLI3522.1>.

- Parkinson, C. L., 2014: Global sea ice coverage from satellite data: Annual cycle and 35-yr trends. *J. Climate*, **27**, 9377–9382, <https://doi.org/10.1175/JCLI-D-14-00605.1>.
- Polvani, L. M., D. W. Waugh, G. J. P. Correa, and S.-W. Son, 2011: Stratospheric ozone depletion: The main driver of twentieth-century atmospheric circulation changes in the Southern Hemisphere. *J. Climate*, **24**, 795–812, <https://doi.org/10.1175/2010JCLI3772.1>.
- Scambos, T. A., J. A. Bohlander, C. A. Shuman, and P. Skvarca, 2004: Glacier acceleration and thinning after ice shelf collapse in the Larsen B embayment, Antarctica. *Geophys. Res. Lett.*, **31**, L18402, <https://doi.org/10.1029/2004GL020670>.
- , G. G. Campbell, A. Pope, T. Haran, A. Muto, M. Lazzara, C. H. Reijmer, and M. R. van den Broeke, 2018: Ultralow surface temperatures in East Antarctica from satellite thermal infrared mapping: The coldest places on Earth. *Geophys. Res. Lett.*, **45**, 6124–6133, <https://doi.org/10.1029/2018GL078133>.
- Schlosser, E., B. Stenni, M. Valt, A. Cagnati, J. G. Powers, K. W. Manning, M. Raphael, and M. G. Duda, 2016: Precipitation and synoptic regime in two extreme years 2009 and 2010 at Dome C, Antarctica—Implications for ice core interpretation. *Atmos. Chem. Phys.*, **16**, 4757–4770, <https://doi.org/10.5194/acp-16-4757-2016>.
- Sinclair, M. R., 1981: Record-high temperatures in the Antarctic—A synoptic case study. *Mon. Wea. Rev.*, **109**, 2234–2242, [https://doi.org/10.1175/1520-0493\(1981\)109<2234:RHTTTA>2.0.CO;2](https://doi.org/10.1175/1520-0493(1981)109<2234:RHTTTA>2.0.CO;2).
- Skansi, M., and Coauthors, 2017: Evaluating highest temperature extremes in the Antarctic. *Eos, Trans. Amer. Geophys. Union*, **98**, <https://doi.org/10.1029/2017EO068325>.
- Thompson, D. C., D. W. Limbert, and G. Manley, 1970: The coreless winter at Scott Base, Antarctica. *Quart. J. Roy. Meteor. Soc.*, **96**, 556–557, <https://doi.org/10.1002/qj.49709640921>.
- Turner, J., and Coauthors, 2004: The SCAR READER project: Towards a high-quality database of mean Antarctic meteorological observations. *J. Climate*, **17**, 2890–2898, [https://doi.org/10.1175/1520-0442\(2004\)017<2890:TSRPTA>2.0.CO;2](https://doi.org/10.1175/1520-0442(2004)017<2890:TSRPTA>2.0.CO;2).
- , and Coauthors, 2009: Record low surface air temperature at Vostok station, Antarctica. *J. Geophys. Res.*, **114**, D24102, <https://doi.org/10.1029/2009JD012104>.
- , T. Maksym, T. Phillips, G. J. Marshall, and M. P. Meredith, 2013: Impact of changes in sea ice advance on the large winter warming on the western Antarctic Peninsula. *Int. J. Climatol.*, **33**, 852–861, <https://doi.org/10.1002/joc.3474>.
- , and Coauthors, 2016: Absence of 21st century warming on Antarctic Peninsula consistent with natural variability. *Nature*, **535**, 411–415, <https://doi.org/10.1038/nature18645>.
- , T. Phillips, G. J. Marshall, J. S. Hosking, J. O. Pope, T. J. Bracegirdle, and P. Deb, 2017: Unprecedented springtime retreat of Antarctic sea ice in 2016. *Geophys. Res. Lett.*, **44**, 6868–6875, <https://doi.org/10.1002/2017GL073656>.
- , and Coauthors, 2019a: The dominant role of extreme precipitation events in Antarctic snowfall variability. *Geophys. Res. Lett.*, **46**, 3502–3511, <https://doi.org/10.1029/2018GL081517>.
- , G. Marshall, K. R. Clem, S. R. Colwell, T. Phillips, and H. Lu, 2019b: Antarctic temperature variability and change from station data. *Int. J. Climatol.*, **40**, 2986–3007, <https://doi.org/10.1002/joc.6378>.
- van den Broeke, M. R., 1998: The semi-annual oscillation and Antarctic climate. Part 1: Influence on near surface temperatures (1957–79). *Antarct. Sci.*, **10**, 175–183, <https://doi.org/10.1017/S0954102098000248>.
- Vavrus, S. J., J. E. Walsh, and W. L. Chapman, 2006: The behavior of extreme cold air outbreaks under greenhouse warming. *Int. J. Climatol.*, **26**, 1133–1147, <https://doi.org/10.1002/joc.1301>.
- Wake, L. M., and S. J. Marshall, 2015: Assessment of current methods of positive degree-day calculation using in situ observations from glaciated regions. *J. Glaciol.*, **61**, 329–344, <https://doi.org/10.3189/2015JogG14J116>.
- Wei, T., Q. Yan, and M. Ding, 2019: Distribution and temporal trends of temperature extremes over Antarctica. *Environ. Res. Lett.*, **14**, 084040, <https://doi.org/10.1088/1748-9326/ab33c1>.
- Zazulie, N., M. Rusticucci, and S. Solomon, 2010: Changes in climate at high southern latitudes: A unique daily record at Orcadas spanning 1903–2008. *J. Climate*, **23**, 189–196, <https://doi.org/10.1175/2009JCLI3074.1>.
- Zhai, P., and X. Pan, 2003: Change in extreme temperature and precipitation over northern China during the second half of the 20th century. *Acta Geogr. Sin.*, **58**, 1–10.
- Zwally, H. J., J. C. Comiso, C. L. Parkinson, D. J. Cavalieri, and P. Gloersen, 2002: Variability of Antarctic sea ice 1979–1998. *J. Geophys. Res.*, **107**, 3041, <https://doi.org/10.1029/2000JC000733>.